

A New Metallicity Calibration for Dwarf Stars with RGU-Photometry

Salih KARAALİ, Selçuk BİLİR

*Istanbul University Science Faculty Department of Astronomy and Space Sciences,
34452 İstanbul-TURKEY
e-mail: karsa@istanbul.edu.tr*

Received 07.12.2001

Abstract

We have adopted the procedure of Carney to obtain a metallicity calibration for dwarfs utilising RGU-photometry. For this purpose we selected 76 dwarfs of different metallicities from Carney and from Strobel et al., and evaluated their $\delta(U-G)$ ultra-violet excess relative to the Hyades by transforming UBV magnitudes to RGU via the metallicity dependent equations of Ak-Güngör. The $\delta_{0.6}/\delta M$ normalized factors of Sandage transform $\delta(U-G)$ excess at any $G-R$ to $\delta \equiv \delta_{1.08}$, i.e. the ultra-violet excess at $G-R = 1.08$ mag, corresponding to $B-V = 0.60$ mag in the UBV-system. Finally, the $(\delta, [Fe/H])$ pairs were shown to be fitted by the equation $[Fe/H] = 0.11 - 2.22 \delta - 7.95 \delta^2$. This calibration covers the metallicity interval $(-2.20, +0.20)$ dex.

Key Words: Metallicity – RGU photometry – Galactic structure

1. Introduction

Metallicity plays an important role in Galactic evolution. Although mean metal-abundances are attributed to the three main Galactic components, i.e. Population I (Thin Disk), Intermediate Population II (Thick Disk), and Extreme Population II (Halo) (cf. Norris [1]), recent work shows that the metallicity distributions for these populations may well be multimodal (Norris [1], Carney [2], Karaali et al. [3]). More important is perhaps the metallicity gradient cited either for populations individually or for a region of the Galaxy. Examples can be found in Reid and Majewski [4], and Chiba and Yoshii [5]. The importance lies in consequences for the formation of the Galaxy, as explained in the following: The existence of a metallicity gradient for any component of the Galaxy means that it formed by dissipative collapse. The pioneers of this suggestion are Eggen, Lynden-Bell, and Sandage [6, ELS]. A discussion of the current status of this model is provided by Gilmore, Wyse, and Kuijken [7]. Many later analyses followed (e.g. Yoshii and Saio [8], Norris, Bessell, and Pickles [9, NBP], Norris [10], Sandage and Fouts [11], Carney, Latham, and Laird [12], Norris and Ryan [13], Beers and Sommer-Larsen [14]). From these works, an alternative picture has emerged, suggesting that the collapse of the Galaxy occurred slowly. This picture was postulated largely on a supposed wide age range in the globular cluster system (Searle and Zinn [15, SZ], Schuster and Nissen [16]). SZ especially argued that the Galactic halo was not formed in an ordered collapse, but from the merger or accretion of numerous fragments, such as dwarf-type galaxies. Such a scenario indicates no metallicity gradient or younger and even more metal-rich objects at the outermost part of the Galaxy. The globular cluster age range suggestion has been disproved by recent analyses (Rosenberg et al. [17]), while the number of young field halo stars has been shown to be extremely small and inconsistent with this model by Unavane, Wyse, and Gilmore [18], Preston and Sneden [19] and Gilmore [20].

A clear metallicity gradient is sensitively dependent on an accurate metallicity determination. In RGU photometry, the calibrations of Buser and Fenkart [21] and Buser et al. [22], calibrated as a function of both G–R colour index and the ultra–violet excess (relative to the zero iso–metallicity line) are used. Correspondingly, the metallicity equation of Carney [23], i.e. $[\text{Fe}/\text{H}] = 0.11 - 2.90 \delta - 18.68 \delta^2$, is preferred in UB–V photometry. The large sample of Carney includes stars of different categories, such as dwarfs, subgiants, and close binaries, allowing the calibration for this relationship to extend down to $[\text{Fe}/\text{H}] = -2.45$ dex. However, it is assumed to be valid only for $[\text{Fe}/\text{H}] \geq -1.75$ dex (Laird, Carney, and Latham [24, LCL], Gilmore, Wyse, and Jones [25]). We decided to contribute to this topic by obtaining a metallicity calibration for dwarfs from RGU photometry, using a method similar to that of Carney [23], and that is the main goal of this paper.

2. The Method

The method consists of applying the procedure of Carney [23] to RGU photometry. Two steps were followed for our purpose: in the first step, UB–V data for 52 and 24 dwarfs taken from Carney [23] and Strobel et al. [26], respectively, are transformed to the RGU system by means of the metallicity dependent conversion equations of Ak–Güngör [27]. The (U–G, G–R) main–sequence of the Hyades, transformed from UB–V to RGU by the same formulae, is used as a standard sequence for ultra–violet excess evaluation. The transformation formulae just cited, or those of Buser [28], may be used to show that the coefficients given by Sandage [29] for UB–V photometry may also be used for the normalization of these photometric excesses, as explained in the following:

The equations which transform U–B and B–V colour indices of a star to the G–R and U–G colour indices are in the form of

$$G - R = a_1(U - B) + b_1(B - V) + c_1 \quad (1)$$

$$U - G = a_2(U - B) + b_2(B - V) + c_2, \quad (2)$$

where a_i , b_i , and c_i ($i = 1, 2$) are parameters to be determined. Let us write Equation (2) for two stars with the same B–V (or equivalently, G–R), i.e. for a Hyades star (H) and for a star (*) whose ultra–violet excess would be normalized,

$$(U - G)_H = a_2(U - B)_H + b_2(B - V) + c_2 \quad (3)$$

$$(U - G)_* = a_2(U - B)_* + b_2(B - V) + c_2. \quad (4)$$

Then, the ultra–violet excess for the star in question, relative to the Hyades star is,

$$(U - G)_H - (U - G)_* = a_2[(U - B)_H - (U - B)_*], \quad (5)$$

or in standard notation,

$$\delta(U - G) = a_2\delta(U - B). \quad (6)$$

Now, for another star with the same metal–abundance $[\text{Fe}/\text{H}]$ but with $B - V = 0.6$ mag, (or its equivalent, $G - R = 1.08$) we get in the same way,

$$\delta(U - G)_{1.08} = a_2 \delta(U - B)_{0.6}. \quad (7)$$

Equations (6) and (7) give,

$$\frac{\delta(U - G)_{1.08}}{\delta(U - G)} = \frac{\delta(U - B)_{0.6}}{\delta(U - B)} = f, \quad (8)$$

where f is the ultra-violet excess conversion factor in question. Hence, $\delta(U-G)$ excess in RGU photometry can be normalised by the same f factors used in UBV photometry. Table 1 gives the normalization factors taken from Sandage [29]. $[\text{Fe}/\text{H}]$ metallicities and UBV data from Carney [23] and Strobel et al. [26], and their corresponding RGU data are given in Table 2a and Table 2b, respectively. Dwarfs in Table 2a are identified according to their spectral types, whereas dwarfs in Table 2b have high surface gravities, i.e. $\log g > 4.0$.

Table 1. Hyades main-sequence de-reddened colour-colour relation, and the normalization factor (f) of Sandage.

$(\mathbf{B-V})_o$	$(\mathbf{U-B})_o$	f	$(\mathbf{B-V})_o$	$(\mathbf{U-B})_o$	f	$(\mathbf{B-V})_o$	$(\mathbf{U-B})_o$	f
0.35	0.03	1.24	0.66	0.20	1.04	0.97	0.78	1.71
0.36	0.03	1.23	0.67	0.22	1.06	0.98	0.80	1.74
0.37	0.02	1.22	0.68	0.23	1.07	0.99	0.82	1.78
0.38	0.02	1.21	0.69	0.25	1.09	1.00	0.84	1.82
0.39	0.01	1.20	0.70	0.25	1.10	1.01	0.86	1.87
0.40	0.01	1.19	0.71	0.27	1.12	1.02	0.88	1.92
0.41	0.01	1.18	0.72	0.29	1.14	1.03	0.90	1.96
0.42	0.01	1.17	0.73	0.30	1.15	1.04	0.93	2.01
0.43	0.00	1.17	0.74	0.33	1.17	1.05	0.94	2.06
0.44	0.00	1.16	0.75	0.34	1.19	1.06	0.96	2.16
0.45	0.00	1.15	0.76	0.36	1.21	1.07	0.97	2.27
0.46	0.01	1.14	0.77	0.38	1.23	1.08	0.98	2.37
0.47	0.01	1.13	0.78	0.40	1.25	1.09	0.99	2.48
0.48	0.02	1.13	0.79	0.42	1.27	1.10	1.01	2.58
0.49	0.03	1.12	0.80	0.43	1.29	1.11	1.03	2.58
0.50	0.03	1.11	0.81	0.45	1.31	1.12	1.05	2.58
0.51	0.04	1.09	0.82	0.47	1.34	1.13	1.07	2.58
0.52	0.05	1.08	0.83	0.49	1.36	1.14	1.08	2.82
0.53	0.06	1.06	0.84	0.52	1.39	1.15	1.10	2.82
0.54	0.07	1.05	0.85	0.54	1.41	1.16	1.12	2.82
0.55	0.08	1.03	0.86	0.56	1.44	1.17	1.14	2.82
0.56	0.09	1.02	0.87	0.58	1.47	1.18	1.15	3.10
0.57	0.10	1.02	0.88	0.60	1.49	1.19	1.16	3.44
0.58	0.11	1.01	0.89	0.62	1.52	1.20	1.17	3.44
0.59	0.12	1.01	0.90	0.64	1.55	1.21	1.18	4.43
0.60	0.13	1.00	0.91	0.66	1.57	1.22	1.19	4.77
0.61	0.14	1.01	0.92	0.68	1.58	1.23	1.19	6.20
0.62	0.16	1.01	0.93	0.70	1.60	1.24	1.20	7.75
0.63	0.17	1.02	0.94	0.71	1.61	1.25	1.21	7.75
0.64	0.18	1.02	0.95	0.74	1.63			
0.65	0.19	1.03	0.96	0.76	1.67			

Table 2a. [Fe/H] metallicities and UBVR data from Carney and the corresponding RGU data. The metallicities in columns 3 and 7 correspond to the adopted values from Carney, and the computed ones by means of equation $[\text{Fe}/\text{H}] = 0.11 - 2.22 \delta_{(1.08)} - 7.95 \delta_{(1.08)}^2$; $\delta_{(1.08)}$ in column 6 is the ultra-violet excess relative to Hyades, reduced to the colour index $G-R = 1.08$, and finally column 8 is the difference of metallicity between columns 3 and 7.

	1	2	3	4	5	6	7	8
Star	B-V	U-B	[Fe/H] _{ad}	G-R	U-G	$\delta_{(1.08)}$	[Fe/H] _c	$\Delta[\text{Fe}/\text{H}]$
HD 2151	0.62	0.11	0.12	1.11	1.46	0.07	-0.10	0.22
HD 10700	0.72	0.21	-0.36	1.22	1.57	0.13	-0.34	-0.02
HD 13555	0.42	-0.07	-0.40	0.87	1.20	0.12	-0.30	-0.10
HD 13974	0.61	0.02	-0.50	1.09	1.33	0.17	-0.53	0.03
HD 16895	0.49	0.00	-0.10	0.95	1.31	0.04	0.00	-0.10
HD 17948	0.44	-0.12	-0.35	0.90	1.15	0.18	-0.58	0.23
HD 19445	0.46	-0.24	-1.92	0.96	1.01	0.38	-1.86	-0.06
HD 20630	0.68	0.19	0.10	1.18	1.56	0.07	-0.10	0.20
HD 20766	0.64	0.07	-0.37	1.13	1.40	0.14	-0.39	0.02
HD 20807	0.60	-0.02	-0.34	1.08	1.29	0.19	-0.63	0.29
HD 20794	0.71	0.22	-0.34	1.21	1.58	0.09	-0.18	-0.16
HD 22879	0.54	-0.08	-0.57	1.01	1.21	0.21	-0.73	0.16
HD 25329	0.86	0.38	-1.33	1.39	1.77	0.36	-1.70	0.37
HD 30649	0.59	0.02	-0.32	1.07	1.34	0.14	-0.39	0.07
HD 30652	0.46	-0.01	0.17	0.91	1.30	0.02	0.06	0.11
HD 39587	0.59	0.08	0.06	1.07	1.42	0.06	-0.07	0.13
HD 63077	0.57	-0.07	-0.80	1.06	1.22	0.25	-0.96	0.16
HD 64090	0.61	-0.12	-1.73	1.12	1.16	0.38	-1.86	0.13
HD 65583	0.70	0.18	-0.62	1.20	1.53	0.12	-0.30	-0.32
HD 69897	0.47	-0.06	-0.52	0.93	1.22	0.14	-0.39	-0.13
HD 72905	0.62	0.07	-0.27	1.10	1.39	0.12	-0.30	0.03
HD 74000	0.43	-0.23	-2.05	0.94	1.02	0.36	-1.70	-0.35
HD 84737	0.62	0.08	-0.04	1.11	1.43	0.10	-0.22	0.18
HD 90508	0.60	0.05	-0.23	1.09	1.39	0.11	-0.26	0.03
HD 101501	0.74	0.23	-0.27	1.24	1.59	0.13	-0.34	0.07
HD 106516	0.44	-0.13	-0.72	0.90	1.14	0.19	-0.63	-0.09
HD 108177	0.43	-0.22	-1.70	0.94	1.03	0.35	-1.63	-0.07
HD 109358	0.59	0.05	-0.04	1.07	1.39	0.09	-0.18	0.14
HD 110897	0.55	-0.03	-0.31	1.02	1.27	0.15	-0.43	0.12
HD 114710	0.58	0.08	0.16	1.06	1.42	0.05	-0.04	0.20
HD 114762	0.52	-0.08	-0.64	0.99	1.21	0.19	-0.63	-0.01
HD 131156	0.77	0.29	-0.13	1.29	1.69	0.16	-0.48	0.35
HD 132142	0.79	0.33	-0.55	1.30	1.71	0.16	-0.48	-0.07
HD 136352	0.64	0.06	-0.49	1.13	1.38	0.16	-0.48	-0.01
HD 141004	0.60	0.10	0.03	1.08	1.45	0.03	0.03	0.00
HD 142860	0.48	-0.03	-0.19	0.94	1.28	0.07	-0.10	-0.09
BD+42° 2667	0.46	-0.20	-1.67	0.97	1.06	0.33	-1.49	-0.18
HD 148816	0.53	-0.07	-0.63	1.00	1.22	0.19	-0.63	0.00

Table 2a. (cont.)

	1	2	3	4	5	6	7	8
Star	B-V	U-B	[Fe/H] _{ad}	G-R	U-G	$\delta_{(1.08)}$	[Fe/H] _c	Δ [Fe/H]
HD 152792	0.65	0.08	-0.38	1.14	1.41	0.15	-0.43	0.05
HD 157089	0.56	-0.01	-0.54	1.03	1.29	0.14	-0.39	-0.15
HD 157214	0.62	0.06	-0.47	1.10	1.38	0.13	-0.34	-0.13
BD+18° 3423	0.48	-0.10	-0.94	0.98	1.18	0.22	-0.79	-0.15
HD 160693	0.58	-0.03	-0.69	1.06	1.27	0.20	-0.68	-0.01
HD 165908	0.52	-0.08	-0.46	0.99	1.21	0.19	-0.63	0.17
BD+41° 3306	0.81	0.34	-0.87	1.34	1.72	0.25	-0.96	0.09
HD 188510	0.61	-0.15	-1.80	1.12	1.12	0.42	-2.18	0.38
HD 195633	0.53	-0.06	-1.10	1.03	1.23	0.20	-0.68	-0.42
HD 201891	0.51	-0.16	-1.42	0.99	1.11	0.30	-1.28	-0.14
HD 203608	0.48	-0.13	-0.68	0.94	1.15	0.21	-0.73	0.05
HD 207978	0.41	-0.15	-0.53	0.86	1.11	0.23	-0.85	0.32
HD 208906	0.50	-0.13	-0.51	0.97	1.15	0.23	-0.85	0.34
HD 217014	0.67	0.20	0.12	1.17	1.57	0.04	0.00	0.12

Table 2b. [Fe/H] metallicities and UBV data from Cayrel de Strobel et al. and their corresponding RGU data. Symbols as in Table 2a.

	1	2	3	4	5	6	7	8
Star	B-V	U-B	[Fe/H] _{ad}	G-R	U-G	$\delta_{(1.08)}$	[Fe/H] _c	Δ [Fe/H]
G 206-34	0.30	-0.31	-2.15	0.80	0.92	0.48	-2.70	0.55
BD+64° 0268	0.64	-0.11	-2.11	1.15	1.17	0.42	-2.18	0.07
HD 74000	0.39	-0.27	-2.06	0.89	0.97	0.39	-1.93	-0.13
HD 181743	0.41	-0.28	-2.04	0.91	0.96	0.40	-2.01	-0.03
BD+42° 3607	0.43	-0.27	-2.01	0.93	0.97	0.42	-2.18	0.17
BD+24° 1676	0.26	-0.28	-2.00	0.77	0.95	0.47	-2.61	0.61
HD 64090A	0.61	-0.13	-2.00	1.12	1.15	0.39	-1.93	-0.07
HD 64090B	0.61	-0.15	-1.86	1.12	1.12	0.42	-2.18	0.32
HD 188510	0.56	-0.12	-1.60	1.07	1.16	0.32	-1.42	-0.18
BD+41° 3931	0.59	-0.13	-1.60	1.00	1.15	0.36	-1.70	0.10
HD 59984	0.53	-0.09	-1.60	1.05	1.19	0.27	-1.09	-0.51
BD+72°0094	0.35	-0.24	-1.30	0.84	1.01	0.35	-1.63	0.33
HD 193901	0.52	-0.14	-1.22	1.01	1.14	0.28	-1.15	-0.07
HD 105837	0.55	-0.06	-1.07	1.05	1.23	0.23	-0.85	-0.22
BD+29° 0366	0.54	-0.12	-0.99	1.03	1.16	0.28	-1.15	0.16
HD 194598	0.47	-0.14	-0.99	0.96	1.14	0.24	-0.90	-0.09
HD 52298	0.45	-0.12	-0.84	0.95	1.16	0.21	-0.73	-0.11
HD 6582	0.69	0.10	-0.71	1.18	1.44	0.20	-0.68	-0.03
HD 65583	0.69	0.17	-0.60	1.18	1.52	0.11	-0.26	-0.34
HD185144	0.77	0.38	-0.23	1.29	1.80	0.03	0.03	-0.26
HD 3765	0.93	0.69	-0.06	1.48	2.19	0.03	0.03	-0.09
HD 149661	0.82	0.50	0.01	1.35	1.95	-0.01	0.14	-0.13
HD 193664	0.57	0.04	0.06	1.05	1.37	0.09	-0.18	0.24
HD 155886	0.85	0.49	0.09	1.39	1.94	0.12	-0.30	0.39

Table 3. Metallicity distribution for 76 stars taken from Carney, and Cayrel de Strobel et al. Mean metallicities (column 3) and mean ultra–violet excesses relative to the Hyades, reduced to the colour–index $G-R = 1.08$ (column 4) are also given. Column 5 gives the number of stars in each metallicity interval.

1	2	3	4	5
[Fe/H]		$\langle[\text{Fe}/\text{H}]\rangle$	$\langle\delta_{1.08}\rangle$	N
-2.20	-2.00	-2.10	0.42	8
-2.00	-1.70	-1.85	0.39	5
-1.70	-1.40	-1.55	0.32	5
-1.40	-1.10	-1.25	0.30	4
-1.10	-0.90	-1.00	0.24	4
-0.90	-0.70	-0.80	0.22	5
-0.70	-0.60	-0.65	0.17	6
-0.60	-0.50	-0.55	0.18	7
-0.50	-0.40	-0.45	0.15	4
-0.40	-0.30	-0.35	0.14	8
-0.30	-0.20	-0.25	0.10	4
-0.20	0.00	-0.10	0.08	6
0.00	0.10	0.05	0.06	6
0.10	0.20	0.15	0.05	4

In the second step, 76 stars (given in Tables 2a and 2b) are separated into 14 metallicity intervals, with different bin sizes, chosen such as to provide an almost equal number of stars in each bin. The least–squares method is used to obtain a calibration between the normalized ultra–violet excess $\delta_{1.08}$ and metallicity [Fe/H] (Table 3). This binning provides equal–weight data for 14 points in Figure 1, which represent the mean metallicities and mean $\delta_{1.08}$ excesses in each metallicity interval in Table 3. The constant term a_o in the equation,

$$[Fe/H] = a_o + a_1\delta_{1.08} + a_2\delta_{1.08}^2 \tag{9}$$

is assumed to be $a_o = 0.11$ for consistency with the metallicity of the Hyades cited by Carney [23]. The least–squares method gives $a_1 = - 2.22$ and $a_2 = - 7.95$ thus,

$$[Fe/H] = 0.11 - 2.22\delta_{1.08} - 7.95\delta_{1.08}^2. \tag{10}$$

The differences between the metallicities evaluated by means of Equation (10) and the original ones, ie.: $\Delta[\text{Fe}/\text{H}]$, (column 8, in Tables 2a and 2b) versus the original metallicities are given in Figure 2. The differences are large only for a few metal–poor stars, while the scatter relative to the line $\Delta[\text{Fe}/\text{H}] = 0.0$ dex is small. Actually, the mean of the differences (for all stars) is only 0.02 dex, while the probable error for the mean is small, p.e. = ± 0.15 dex, indicating that the new calibration can be used with good accuracy.

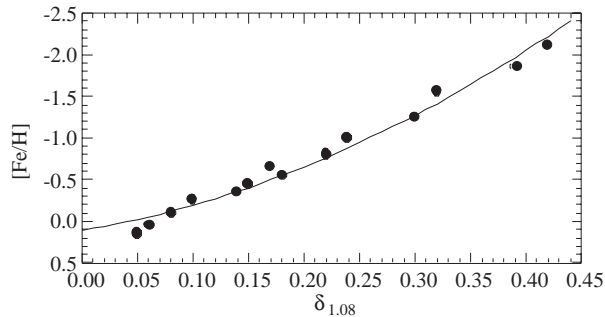


Figure 1. [Fe/H] metallicity versus normalized $\delta_{1.08}$ ultra–violet excess for RGU photometry.

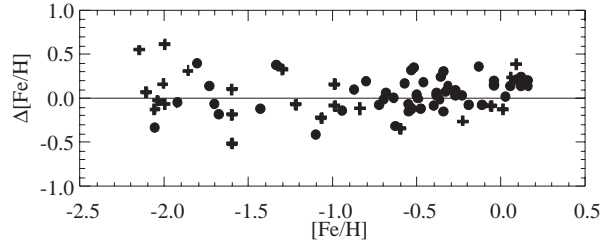


Figure 2. $\Delta[\text{Fe}/\text{H}]$ versus metallicity, where $\Delta[\text{Fe}/\text{H}]$ is the difference between the original metallicities and the evaluated ones, utilising the new calibration, $[\text{Fe}/\text{H}] = 0.11 - 2.22 \delta_{1.08} - 7.95 \delta_{1.08}^2$. Symbols: (●) stars from Table 2a, and (+) stars from Table 2b.

3. Discussion

The procedure used by Buser and Fenkart [21] for metallicity determination of a dwarf star is based on the combination of its ultra-violet excesses relative to Population I (zero metallicity) dwarfs and its G–R colour index. This method requires effort, while the calibration given here is more practical. Although the procedure in the work of Buser and Fenkart [21] provides a larger metallicity interval than ours, i.e. down to $[\text{Fe}/\text{H}] = -3.0$ dex and $[\text{Fe}/\text{H}] = -2.2$ dex, respectively, the number of stars with $[\text{Fe}/\text{H}] < -2.2$ dex in our Galaxy is small, so that this new calibration does not provide any significant restriction in metallicity analyses concerned with Galactic structure.

Comparison of our new calibration with that of Carney [23] shows that our calibration has some advantages, probably due to our use of additional metal-poor stars, as explained in the following: **(1)** Our new calibration is available for stars with $[\text{Fe}/\text{H}] \geq -2.20$ dex, whereas the earlier calibration is limited to $[\text{Fe}/\text{H}] \geq -1.75$ dex. **(2)** Calibration of the relationship between $[\text{Fe}/\text{H}]$ and normalized UV-excess, $\delta_{1.08}$, in this work is steeper than the corresponding one in the work of Carney [23]. Although the figure from Carney is not given here, this can be deduced by the comparison of the scales in UV-excess in the two works. This new relation provides more accurate metallicities. **(3)** The diagram $\Delta[\text{Fe}/\text{H}]$ versus original metallicities in our work (Figure 2) is better defined than the one for the data of Carney (Figure 3), where $\Delta[\text{Fe}/\text{H}]$ is the difference between the original metallicities and the derived ones from the corresponding equation. Specifically, the mean and standard deviation for $\Delta[\text{Fe}/\text{H}]$, for all stars, in our work are $\langle \Delta[\text{Fe}/\text{H}] \rangle = 0.02$ dex, and $s = \pm 0.22$ dex, respectively, whereas they are $\langle \Delta[\text{Fe}/\text{H}] \rangle = 0.03$ dex, and $s = \pm 0.27$ dex for the data evaluated via the formula of Carney, for stars only with $\Delta[\text{Fe}/\text{H}] < +1.00$ dex (four stars with $\Delta[\text{Fe}/\text{H}] \geq +1.00$ dex in Figure 3 are not included for these evaluations). That is, we have provided a valuable tool for the analysis of the galactic metallicity distribution function in our new calibration.

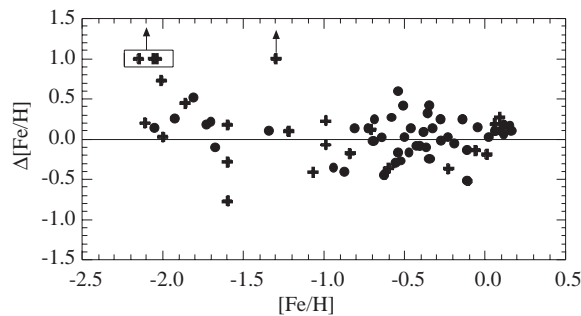


Figure 3. $\Delta[\text{Fe}/\text{H}]$ versus metallicity, where $\Delta[\text{Fe}/\text{H}]$ is the difference between the original metallicities and that derived from Carney's equation, i.e. $[\text{Fe}/\text{H}] = 0.11 - 2.90 \delta_{0.6} - 18.68 \delta_{0.6}^2$. Symbols as in Figure 2.

Acknowledgement

We would like to thank the anonymous referees for their comments.

References

- [1] J. E. Norris, *ASP Conf. Ser.*, **92**, (1996), 14.
- [2] B. W. Carney, *Proceedings of the 35th Liège Int. Astrophys. Coll., July 5 – 8, 1999*, (2000) 287.
- [3] S. Karaali, Y. Karataş, S. Bilir, S. G. Ak, & G. Gilmore, *Proceedings of the 35th Liège. Int. Astrophys. Coll., July 5 – 8, 1999*, (2000), 353.
- [4] N. Reid & S. R. Majewski, *ApJ*, **409**, (1993), 635.
- [5] M. Chiba & Y. Yoshii, *AJ*, **115**, (1998), 168.
- [6] O. J. Eggen, D. Lynden – Bell, & A. R. Sandage, *ApJ*, **136**, (1962), 748 (ELS).
- [7] G. Gilmore, R. F. G. Wyse, & K. Kuijken, *ARAA*, **27**, (1989), 555.
- [8] Y. Yoshii & H. Saio, *PASJ*, **31**, (1979), 339.
- [9] J. E. Norris, M. S. Bessell, & A. J. Pickles, *AJ*, **58**, (1985), 463 (NBP).
- [10] J. E. Norris, *ApJS*, **61**, (1986), 667.
- [11] A. R. Sandage & G. Fouts, *AJ*, **93**, (1987), 74.
- [12] B. W. Carney, D. W. Latham, & J. B. Laird, *AJ*, **99**, (1990), 572.
- [13] J. E. Norris & S. G. Ryan, *ApJ*, **380**, (1991), 403.
- [14] T. C. Beers & J. Sommer – Larsen, *ApJS*, **96**, (1995), 175.
- [15] L. Searle & R. Zinn, *ApJ*, **225**, (1978), 357 (SZ).
- [16] W. J. Schuster & P. E. Nissen, *A&A*, **222** (1989) 69.
- [17] A. Rosenberg, I. Saviane, G. Piotto, & A. Aparico, *AJ*, **118**, (1999), 2306.
- [18] M. Unavane, R. F. G. Wyse, & G. Gilmore, *MNRAS*, **278**, (1996), 727.
- [19] G. W. Preston & C. Sneden, *AJ*, **120**, (2000), 1014.
- [20] G. Gilmore, *JBAA*, **110**, (2000), 42.
- [21] R. Buser & R. P. Fenkart, *A&A*, **239** (1990) 243.
- [22] R. Buser, Y. Karataş, Th. Lejeune, J. X. Rong, P. Westa, & S. G. Ak, *A&A*, **357**, (2000), 988.
- [23] B. W. Carney, *ApJ*, **233**, (1979), 211.
- [24] J. B. Laird, B. W. Carney, & D. W. Latham, *AJ*, **95**, (1988), 1843 (LCL).
- [25] G. Gilmore, R. F. G. Wyse, & J. B. Jones, *AJ*, **109**, (1995), 1095.
- [26] G. C. Strobel, C. Soubiran, E. D. Friel, N. Ralite, & P. Francois, *A&AS*, **124**, (1997), 299.
- [27] S. Güngör Ak, *Ph. D. Thesis, Science Institute, University of Istanbul*, (1995).
- [28] R. Buser, *A&A*, **62**, (1978), 425.
- [29] A. R. Sandage, *ApJ*, **158**, (1969), 1115.